Size control of vapor bubbles on a silver film by a tuned CW laser

Y. J. Zheng, Y. Wang, H. Liu, C. Zhu, S. M. Wang et al.

Citation: AIP Advances **2**, 022155 (2012); doi: 10.1063/1.4730929
View online: http://dx.doi.org/10.1063/1.4730929
View Table of Contents: http://aipadvances.aip.org/resource/1/AAIDBI/v2/i2
Published by the American Institute of Physics.

Related Articles

Period adding cascades: Experiment and modeling in air bubbling
Chaos 22, 013135 (2012)

Enhancement of critical heat flux in pool boiling using atomic layer deposition of alumina
Appl. Phys. Lett. 100, 053120 (2012)

Monte Carlo predictions of phase equilibria and structure for dimethyl ether + sulfur dioxide and dimethyl ether + carbon dioxide
J. Chem. Phys. 136, 044514 (2012)

On the low frequency loss peak in the dielectric spectrum of glycerol
J. Chem. Phys. 135, 094502 (2011)

On the effect of surface roughness height, wettability, and nanoporosity on Leidenfrost phenomena
Appl. Phys. Lett. 98, 083121 (2011)

Additional information on AIP Advances

Journal Homepage: http://aipadvances.aip.org
Journal Information: http://aipadvances.aip.org/about/journal
Top downloads: http://aipadvances.aip.org/most_downloaded
Information for Authors: http://aipadvances.aip.org/authors

ADVERTISEMENT

Downloaded 19 Jun 2012 to 222.94.46.201. All article content, except where otherwise noted, is licensed under a Creative Commons Attribution 3.0 Unported license.
See: http://creativecommons.org/licenses/by/3.0/

Size control of vapor bubbles on a silver film by a tuned CW laser

Y. J. Zheng, Y. Wang, H. Liu,[a] C. Zhu, S. M. Wang, J. X. Cao, and S. N. Zhu
National Laboratory of Solid State Microstructures and Department of Physics, Nanjing University, Nanjing 210093, People's Republic of China

(Received 5 March 2012; accepted 2 June 2012; published online 19 June 2012)

A vapor bubble is created by a weakly focused continuous-wave (CW) laser beam on the surface of a silver film. The temporal dynamics of the bubble is experimentally investigated with a tuned incident laser. The expansion and contraction rates of the vapor bubble are determined by the laser power. The diameter of the vapor bubble can be well controlled through tuning the laser power. A theory model is given to explain the underlying physics in the process. The method reported will have some interesting applications in micro-fluidics and bio-techniques. *Copyright 2012 Author(s). This article is distributed under a Creative Commons Attribution 3.0 Unported License*. [http://dx.doi.org/10.1063/1.4730929]

In a closed container, heating liquid above its boiling point using a hot surface introduces some complex boiling phenomena in the superheating process. These phenomena include natural convection, nucleate boiling, transition boiling, and film boiling. All these effects have been studied intensively and reviewed by Rohsenow,[1] Dhir,[2] Carey[3] and Lin.[4] In these effects, vapor bubble is a very common phenomenon. Numerous studies have been conducted over the past 50 years to understand the formation of vapor bubble.[4–8] Some of these studies investigated the physics of bubble formation and controlling the size of the bubble in microscale devices using micro-resistive heaters.[7,8] In recent years, vapor bubble actuated by laser has attracted considerable interest.[9–14] For examples, thin film heating by a laser has been used to steering the motion of the bubble.[9–11] In practical situations, an individual vapor bubble is usually subjected to various forces such as buoyancy, surface tension, contact pressure forces, etc., which make the creation, growth, departure, and thermal collapse of the vapor bubble highly complex. The size of bubble will play an important role in some related applications. To date, controlling the growth and size of a bubble based on optical method remains a challenge and interesting topic.

In the current study, we investigate the dynamics of a vapor bubble created in a micro-sandwiched water sheet on silver film using a CW laser. Because of the enhanced photothermal effect of the silver film, the bubble can be efficiently created with low input laser power. Confined in a 100 μm thick liquid cell, the generated vapor bubble grows continually for tens of minutes without thermal collapse. The expansion and contraction rates of the bubble can be manipulated by changing the laser power and thickness of the silver film. The steady states of the vapor bubble develop because of the tuning of the laser power, in which the diameter of the bubble can be well controlled at our will.

Figure 1(a) shows the experimental setup, which includes three parts: the liquid cell, laser system, and micro-imaging system. Figure 1(b) shows that the liquid cell consists of a d = 100 μm thick water sheet sandwiched between a glass cover (thickness, 200 μm) and SiO_2 substrate (thickness, 0.5 mm). The silver film is sputtered onto the SiO_2 substrate surface. A very thin Ge film is sputtered between SiO2 substrate and Ag film. As the Ge film is very thin (about several nanometer), the Ge film is not continuous and many Ge nanoparticles are formed on the substrate. This

[a]liuhui@nju.edu.cn; URL: http://dsl.nju.edu.cn/mpp

 © Author(s) 2012

Downloaded 19 Jun 2012 to 222.94.46.201. All article content, except where otherwise noted, is licensed under a Creative Commons Attribution 3.0 Unported license.
See: http://creativecommons.org/licenses/by/3.0/

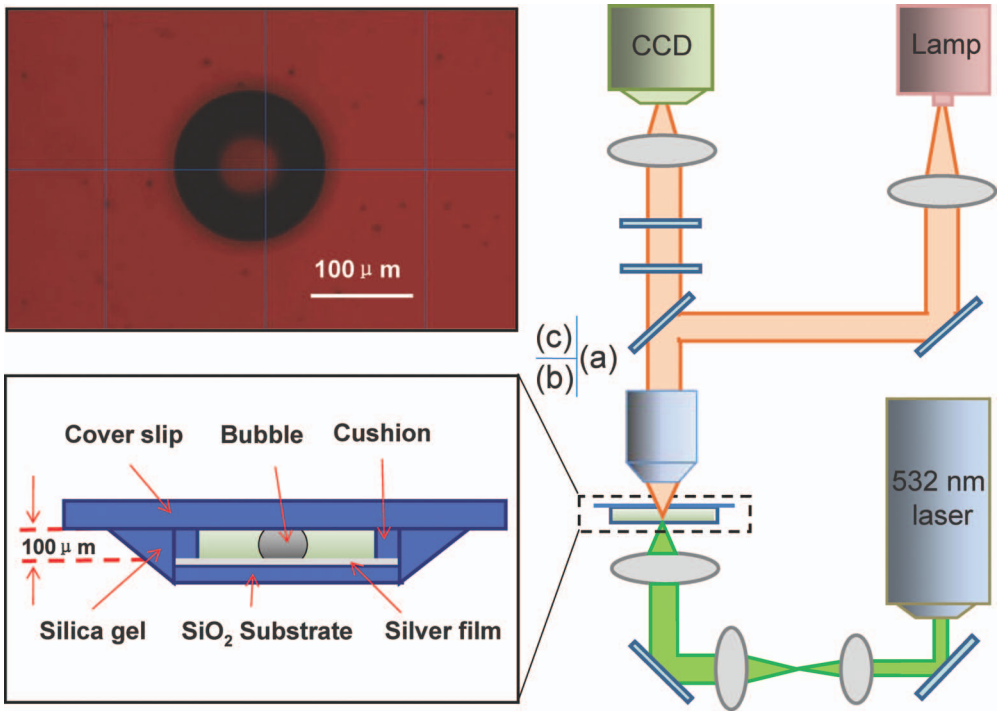

FIG. 1. (a) Experiment setup to study the temporal evolution of the vapor bubble; (b) sketch of liquid cell (not to scale); (c) a picture of a vapor bubble created in the micro-sandwiched water sheet.

TABLE I. The measured threshold power to create vapor bubble for samples with difference thickness of the silver film.

Thickness (nm)	100	300	500	1000
Threshold power (mW)	232± 5.5%	222± 6.5%	317± 3.6%	324± 4.3%

will increase the roughness of the interface between glass substrate and silver film. To generate bubbles, a 532 nm CW laser beam is expanded, collimated, and focused (beam waist, 106 μm) into a liquid cell, with the focusing plane located inside the silver film. The dynamics of the bubbles are illuminated by collimated white light and imaged by a charge coupled device camera with a microscope objective (Zeiss Epiplan 5X /0.13 HD Microscope Objective) [Fig. 1(c)]. A color filter and an attenuator are placed in front of the camera to eliminate the transmitted green laser.

When a 250 mW laser beam is focused onto the silver film, the silver film is quickly heated up because of the efficient absorption of the laser power. The heated silver film can raise the temperature of water above the superheat limit in a very short period. Once this limit is reached, a violent phase explosion occurs, creating a vapor bubble at the interface between water and the silver film. Here, the focusing spot of laser beam behaves like a point heat source, which input energy into bubbles continually and make them expand. In the process, the bubble is firmly attached onto the heating substrate. Once its diameter exceeds the thickness of water sheet, the top of bubble will reach the glass cover slip and its shape is changed from a complete sphere to a truncated sphere.

We use several samples with different silver film thicknesses: 100, 300, 500, and 1000 nm. The threshold laser powers required to create the vapor bubbles for these samples are given in Table I. The different thicknesses correspond to different threshold powers. When the silver film is too thin, most of the laser energy passes through the film and cannot be transformed into heat. Conversely, when the silver film is too thick, a large mass of laser energy is dissipated before it reaches the interface between water and the silver film. Therefore, there exists an optimal thickness of the silver

Downloaded 19 Jun 2012 to 222.94.46.201. All article content, except where otherwise noted, is licensed under a Creative Commons Attribution 3.0 Unported license.
See: http://creativecommons.org/licenses/by/3.0/

TABLE II. The absorptance and reflectance of samples with and without Ge film.

Samples	Ag film with Ge film		Ag film without Ge film		SiO_2
Thickness of Ag film (nm)	100	300	100	300	0
Reflectance (%)	15.3	13.3	67.4	81.6	9.49
Absorptance (%)	84.17	86.25	31.9	17.65	0.026

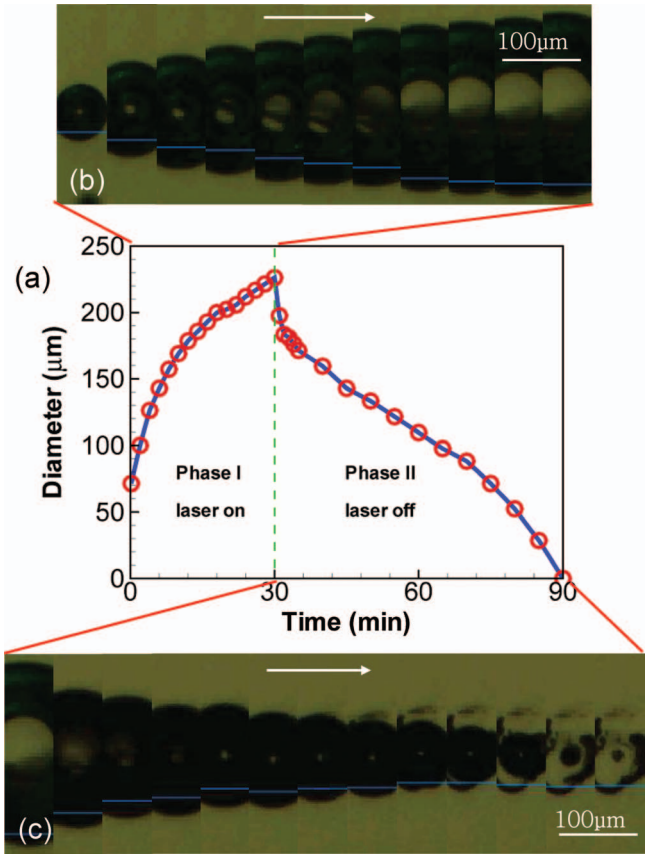

FIG. 2. (a) The temporal evolution of diameter of the vapor bubble with laser on (phase I) and laser off (phase II); (b) the pictures taken for the expanding bubble in phase I (3 min per shot); (c) the pictures taken for the shrinking bubble in phase II (5 min per shot).

film for bubble creation, which corresponds to minimum threshold power P_{th}. In our experiment, the optimal thickness of the silver film is around 300 nm, with threshold power $P_{th} = 222$ mW (Table I).

In the experiment, we compared the absorptance and reflectance of green laser passing through the samples with and without Ge film, which are presented in Table II. It can be seen that for the absorptance of sample with Ge film is about 85%-, which is quite larger than the sample without Ge film (about 30%). In the experiment, for the sample without Ge film, the vapor bubble cannot be created even with the highest power laser available in our lab. However, for the sample with Ge film, the bubble can be created much more easily. Then from the above comparison, we can conclude that the Ge film can enhance the absorption of laser and makes the creation of vapor bubble much easier.

After being created, the vapor bubble can expand or shrink under different input laser powers. Figure 2 shows the time evolution of the diameter of the vapor bubble at an input laser power of

Downloaded 19 Jun 2012 to 222.94.46.201. All article content, except where otherwise noted, is licensed under a Creative Commons Attribution 3.0 Unported license.
See: http://creativecommons.org/licenses/by/3.0/

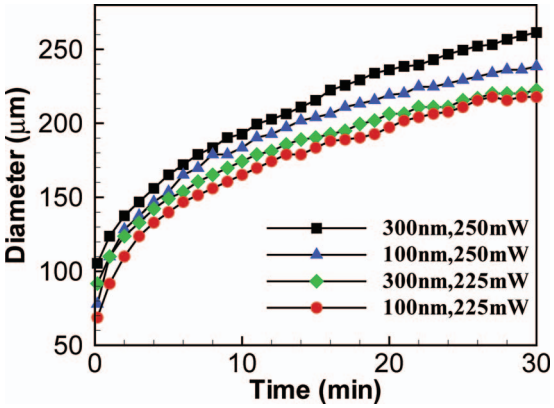

FIG. 3. The expansion process of vapor bubble under difference laser power and thickness of the silver film.

250 mW and a silver film thickness of 300 nm. Initially, a bubble is created with an initial diameter of 71 μm. This process could not be thoroughly replicated in the experiment because the bubble rapidly formed beyond the time resolution allowable in our camera. After its creation, the bubble expands for half an hour with the incident laser power maintaining at 250 mW, shown in Phase I of Fig. 2(a). The bubble exhibits rapid expansion at the beginning of Phase I and expansion slows down at the end of this phase. Phase II in Fig. 2(a) represents the sequential contraction of the bubble after the incidence laser is turned off. The bubble contracts rapidly at the beginning and undergoes a relatively smooth contraction process before it eventually collapses and disappears. The entire process of bubble birth, expansion, and contraction in the experiment is recorded and presented in Figs. 2(b) and 2(c). For the two silver films of different thickness 100 and 300 nm, the evolution curves of the bubble are compared in Fig. 3. Two laser powers 225 mW and 250 mW are used with the size of focusing spot maintained as 106 μm. The results show, with the same input laser, the bubble on the 300 nm thick film is larger than the bubble on 100 nm thick film. For the same film, the size of bubble produced by 250 mW laser is always larger than that by 225 mW laser.

The temperature of the vapor T_v as function of time can be described by the time dependent heat transfer equation:[15,16]

$$\rho_v C_v \frac{\partial T_v}{\partial t} = \alpha I - [\nabla\cdot(-k\nabla T) + S_1\mu_1(T_v - T_{\text{cover}}) + S_2\mu_2(T_v - T_{water})] = Q_{input} - Q_{dissipation}, \quad (1)$$

where ρ_v and C_v are the density and the heat capacity of the vapor. On the right side of equation (1), the first term describes the heating power of silver film determined by absorption coefficient α and laser beam's intensity I. The second term describe the heat diffusion of silver film with a thermal conductivity k. The third and fourth term represents the energy exchange between the vapor bubble and the glass cover, the vapor bubble and surrounding water respectively, with μ_1 and μ_2 being the heat transfer index. S_1 and S_2 are the area of bubble-glass interface and bubble-water interface respectively. In the whole process, the temperature of glass cover slip T_{cover} and water T_{water} are supposed to be unchanged. We assume that the bubble is in a thermodynamical equilibrium process, satisfying the relation $P_v V_v = nRT_v$, where P_v is the vapor pressure inside the bubble, V_v is the volume of the bubble, n is number of H_2O molecules and R is universal gas constant. In our experiment, the pressure inside the bubble should be always equal the pressure outside. As the external pressure is unchanged in our experiment setup, the bubble is actually in an isobaric process: $V_v/nT_v =$ constant. From this relation, the size of the bubble is determined by T_v and we could manipulate the size of the bubble through changing the temperature.

The incident laser beam transfers the energy to the bubble through the silver film. Simultaneously, the bubble dissipates energy into the water and glass cover slip. When $Q_{input} > Q_{dissipation}$, T_v and n are increased, which make the volume of the bubble expand, as shown in Phase I of Fig. 2(a). As the bubble expands, S_1 and S_2 are enlarged and $Q_{dissipation}$ is increased. As a result, the expanding

Downloaded 19 Jun 2012 to 222.94.46.201. All article content, except where otherwise noted, is licensed under a Creative Commons Attribution 3.0 Unported license.
See: http://creativecommons.org/licenses/by/3.0/

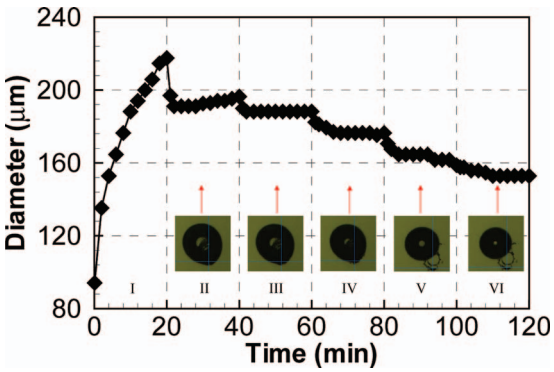

FIG. 4. Black dotted line: the change of vapor bubble when laser power is tuned; Inset: the pictures for the bubbles under different incident power.

rate of the bubble is slowed down [Phase I, Fig. 2(a)]. When $Q_{input} < Q_{dissipation}$, T_v and n are decreased, which make the volume of the bubble shrink, as shown in Phase II of Fig. 2(a). At the beginning of Phase II, the bubble shrinks rapidly because of larger $Q_{dissipation}$. but a decrease of S_1 and S_2 will reduce the value of $Q_{dissipation}$. This will slow down the shrinking speed [Phase II, Fig. 2(a)].

As was discussed above, when $Q_{input} < Q_{dissipation}$, the vapor bubble will shrinks, and $Q_{dissipation}$ will be decreased. When the condition $Q_{input} = Q_{dissipation}$ is satisfied and the bubble will stop shrinking and its size will stabilize. For different input energy Q_{input}, we can obtain the stable bubbles with different size. In the following, we will prove this hypothesis. Firstly, we focus a 300 mW laser beam onto the 300 nm thick silver film for 20 min to obtain a 217 μm bubble [Phase I, black line in Fig. 4]. We then sequentially reduce the laser power to 150, 100, 50, 5, and 0.5 mW step by step. The duration allotted for each incident power is 20 min. As expected, stable states of the bubbles of different size are obtained for different powers. The results are presented as Phases II–VI of the black line in Fig. 4. The images of the bubbles for each stable state are shown as insets in Fig. 4. For incident powers 150, 100, 50, 5, and 0.5 mW, the corresponding stable diameters of the bubble are 191.2, 188.2, 176.4, 164.7, and 152.9 μm, respectively (blue line, Fig. 4). These results show that the size of the bubble can easily be controlled by tuning the laser power.

In conclusion, we have experimentally demonstrated that a single vapor bubble can be produced and well controlled in a micro-sandwiched water sheet by a tuned CW laser. With the help of a thin Ge film, the absorption light by silver is enhanced and the bubble is efficiently created with a CW laser. The threshold laser power for bubble generation depends on the thickness of the silver film. The bubble expands if the input laser power is higher than the dissipation and contracts if the input power is lower than the dissipation. When the laser power equals the dissipation, the bubble is in a stable state and its size is unchanged. By tuning the laser power, the size of the bubble can be completely controlled. The proposed method is a simple and efficient way to create stable and controllable vapor bubbles. The controllable bubbles reported in this work will have some interesting applications in related field. Firstly, as the refractive index of the vapor in the bubble is less than the surrounding water, the vapor bubble can be used as an effective concave lens. Actually, the bubble can be regarded as an inverse structure of droplet, which can be used as a tunable microlenses.[17,18] Secondly, the vapor bubble can be used as a bubble valve, which can be applied to controlling microfluids in channels or biochips[19–21] Another useful application reported recently by us,[22] is to manipulating the microparticles with the laser induced bubble. The microparticles can be attracted to bubble through strong convection flow. Through steering the bubble by laser, we can direct-write micropatterns on a metal film with accumulate particles.

This work was financially supported by the National Natural Science Foundation of China (No. 11021403, 11074119 and 60990320), and by the National Key Projects for Basic Researches of China (No. 2010CB630703, 2012CB921500 and 2012CB933501).

Downloaded 19 Jun 2012 to 222.94.46.201. All article content, except where otherwise noted, is licensed under a Creative Commons Attribution 3.0 Unported license.
See: http://creativecommons.org/licenses/by/3.0/

[1] W. M. Rohsenow, Annu. Rev. Fluid Mech. **3**, 211–236 (1971).
[2] V. K. Dhir, Annu. Rev. Fluid Mech. **30**, 365–401 (1998).
[3] V. P. Carey, *Liquid-Vapor Phase-Change Phenomena* (Routledge, New York, 1992).
[4] L. Lin, Nanoscale and Microscale Thermophysical Engineering **2**, 71–85 (1998).
[5] K. Forster and N. Zuber, J. Appl. Phys. **25**, 474–478 (1954).
[6] S. W. J. Welch, Int. J. Heat Mass Tran. **41**, 1655–1666 (1998).
[7] L. Lin, A. P. Pisano, and V. P. Carey, Journal of Heat Transfer **120**, 735 (1998).
[8] J.-H. Tsai and L. Lin, Journal of Heat Transfer **124**, 375 (2002).
[9] K. T. Kotz, K. A. Noble, and G. W. Faris, Applied Physics Letters **85**, 2658 (2004).
[10] R. H. Farahi, A. Passian, S. Zahrai, A. L. Lereu, T. L. Ferrell, and T. Thundat, Ultramicroscopy **106**, 815–821 (2006).
[11] A. T. Ohta, A. Jamshidi, J. K. Valley, H.-Y. Hsu, and M. C. Wu, Applied Physics Letters **91**, 074103 (2007).
[12] R. A. Taylor, P. E. Phelan, T. Otanicar, R. J. Adrian, and R. S. Prasher, Appl. Phys. Lett. **95**, 161907 (2009).
[13] W. Wagner, A. Sokolow, R. Pearlstein, and G. Edwards, Appl. Phys. Lett. **94**, 013901 (2009).
[14] J. Neumanna and R. Brinkmann, Appl. Phys. Lett. **93**, 033901 (2008).
[15] J. C. Ramirez, E. R. Aboytes, A. E. Martinez, O. B. Pantaleon, A. R. Martinez, N. Korneev, and R. R. Garcia, Opt. Express **18**, 8735–8742 (2010).
[16] D. Turlajs, V. Grivvovs, and S. Yaundalders, *5th WSEAS Int. Conf. on Heat and Mass transfer (HMT'08)*, pp. 80–82 (2008).
[17] R. Won, Nature Photonics **5**, 578 (2011).
[18] P. Fei, Z. He, C. H. Zheng, T. Chen, Y. F. Men, and Y. Y. Huang, Lab Chip **11**, 2835–2841 (2011).
[19] O. Graydon, Nature Photonics **5**, 256 (2011).
[20] K. Zhang, A. Q. Jian, X. M. Zhang, Y. Wang, Z. H. Li, and H. Y. Tam, Lab Chip **11**, 1389–1395 (2011).
[21] C. F. Tsou and C. H. Huang, Microelectromechanical systems **18**, 852–859 (2009).
[22] Y. J. Zheng, H. Liu, Y. Wang, C. Zhu, S. M. Wang, J. X. Cao, and S. N. Zhu, Lab on a Chip **11**, 3816–3820 (2011).

Downloaded 19 Jun 2012 to 222.94.46.201. All article content, except where otherwise noted, is licensed under a Creative Commons Attribution 3.0 Unported license.
See: http://creativecommons.org/licenses/by/3.0/